Regional coastal flood risk assessment for a tidally dominant, natural coastal setting: North Norfolk, southern North Sea

E.K. Christie[a], T. Spencer[a], D. Owen[b], A. McIvor[a], I. Möller[a], C. Viavattene[b]

[a] *Cambridge Coastal Research Unit, Department of Geography, University of Cambridge, Cambridge, UK*
[b] *Flood Hazard Research Centre, Middlesex University, London, UK*

Abstract

A Coastal Risk Assessment Framework (CRAF) provides two levels of coastal risk and vulnerability assessment, by combining information on the spatially variable hazard and exposure. In Phase 1, areas of greatest risk or 'hotspots' are identified. In Phase 2, these hotspots are then analysed in greater detail to identify both direct and indirect extreme event impacts. This approach was applied to the barrier coastline of North Norfolk, eastern England. The CRAF identified high risk coastal hotspots on the basis of both hazard impacts (swash regime (tide + surge + wave runup) and overwash/terrestrial inundation regimes) from a 1 in 115 year return period storm and a range of land use, infrastructure, economic and social vulnerability indicators. Hazard extents and hazard severity, in some locations modified by the presence of intertidal saltmarsh, were calculated for 45, 1-2 km wide sections along the topographically complex coast. When combined with five exposure indicators, eight hotspots were identified along the 45 km long frontage. In a 2nd phase, two of these hotspots, one a chain of small villages (Brancaster/Brancaster Staithe/Burnham Deepdale) and one a small town (Wells-next-the-Sea), were compared in more detail using a suite of coastal inundation and impact assessment models to determine both direct and indirect impacts. Hazards at this higher resolution were calculated using

*Corresponding author
Email address: ekc28@cam.ac.uk (E.K. Christie)

Postprint submitted and accepted to Elsevier *May 22, 2017*

the 1D process-based XBeach model and the 2D LISFLOOD inundation model. Vulnerability to the hazards was calculated using the INDRA (Integrated Disruption Assessment) model with comparison of the two hotspots through the use of a Multi Criteria Analysis (MCA). The selection of hazard hotspots and comparison of hotspots using these techniques allows areas at greatest risk to be identified, of vital importance for coastal management and resource allocation.
Keywords: storm surge flooding, wave runup, wave overwash, XBeach, LISFLOOD, barrier islands, vulnerability, coastal tourism, Multi Criteria Analysis

1. Introduction

On bathymetrically and topographically complex barrier island coastlines, records of storm surge impacts often show considerable local variability at the populated coast (Spencer et al., 2015). This variability can determine local patterns of flood impacts on the linearly-dispersed rural and small urban (population $< 5,000$) settlements characteristic of back-barrier locations. For regional authorities faced with inadequate and reducing budgets, identifying the sites of greatest vulnerability to coastal flooding allows scarce resources for disaster risk reduction to be most effectively deployed. Applying complex modelling approaches along a regional coast may not be resource efficient, necessitating an initial assessment process. In the complex coastal domain this initial assessment must take into account spatial variability in topography, hydrodynamic forcing and exposure.

A common approach to coastal vulnerability assessment is through a coastal vulnerability index. On a very large scale the coastline can be categorised and a vulnerability index created based on the sensitivity of sections of the coast to hazards (Abuodha and Woodroffe, 2006). The sensitivity of the coast can also be combined with politico-administrative and socio-economic indicators to relate hazard susceptibility to exposure and resilience (Balica et al., 2012). McLaughlin and Cooper (2010) highlighted the importance of scale in choosing

the relevant variables to include in coastal vulnerability indicators. To aid decision making and coastal management, these variables can be weighted based on importance by stakeholders Torresan et al. (2012). Analysis of historic hydrodynamic conditions and storm impacts can be used with simple empirical formulae to assess the probability of event occurrence and hazards can then be related to risk through vulnerability thresholds (Armaroli et al., 2012). Torresan et al. (2008) noted the importance of inclusion of environmental variables to more accurately predict coastal susceptibility, such variables include geomorphology, wetlands and vegetation cover.

To improve upon existing coastal risk assessment methods, we combine some of the above approaches of coastal vulnerability assessment. The Coastal Risk Assessment Framework (CRAF) provides a standardized assessment of coastal risk at 2 levels of scale and model complexity. In CRAF Phase 1 a coastal index approach is used, which provides an initial screening process applied on a regional scale. We demonstrate how the spatial variability of coastal hazards can be calculated using historical hydrodynamic conditions and simple empirical formulae (Holman, 1986; Stockdon et al., 2006; Pullen et al., 2007; Donnelly, 2008). We also present new techniques of incorporating the natural coastal defence of intertidal wetlands in the calculation of hazards. The hazards are combined with spatial variable exposure components in a coastal vulnerability indicator to identify coastal hotspots of risk (Viavattene et al., 2015). In CRAF Phase 2, these hotspots are then compared on a smaller scale in more detail. A chain of coastal inundation and impact assessment models are used to determine both direct and indirect impacts. The vulnerability indicators are weighted by expert judgement to complete a Multi Criteria Analysis (MCA).

In this paper we present the CRAF framework for the North Norfolk coast, eastern England. Section 2 describes the case study site, section 3 presents the first phase of the CRAF framework, the identification of risk hotspots. In section 4, the 2nd phase of the CRAF framework is presented, the comparison of the hotspots. Finally, in section 5 we discuss the results and present our conclusions.

2. Study Site

The 45 km long North Norfolk coast (Figure 1) is macro-tidal (mean spring tidal range of 6.6 m in the west at Hunstanton, reducing eastwards to 4.7 m at Cromer) but characterised by a moderate to low wave climate (monthly mean significant wave heights (2006 - 2009): 0.36 and 0.80 m at Scolt Head Island (5 m water depth), and Cley (7 m) respectively (Environment Agency, 2014)). The wave climate recorded at these nearshore wave buoys is largely uni-directional, with a dominant wave direction of North - North East, and uni-modal. The nearshore wave peak periods show a dominance of locally generated wind waves (3-5 s peak period). Swell waves occur occasionally during stormier periods caused by low pressure to the North. The combination of high tidal range and low offshore slopes has allowed the development of extensive subtidal and intertidal mudflats, sandflats seaward of large gravel barriers (Scolt Head Island, Blakeney Point), back-barrier mudflats, tidal channels and saltmarshes. Landward margins are characterised by reclaimed saltmarsh (freshwater marsh) and, locally, by reedbeds and sand dunes (some with plantation forest). Within the case study site there are 2 towns and 14 villages, some with small harbours and quays. Whilst predominantly agricultural, the coast is an important area for nature conservation, with walking and birdwatching activities bringing tourism to the coast year round.

The southern North Sea is susceptible to storm surges which can elevate peak water levels over 1 m above the predicted tidal levels; there have been 21 such events, of varying severity, since 1883 (Brooks et al., 2016). Landscape impacts of major surges are: landward washover of beach and dune sands onto back-barrier marshes; cliffing and retreat of coastal dunes; breaching of the major gravel barrier between Cley and Salthouse; flooding of freshwater marshes and ponding of saltwater; loss of invertebrate populations and 'washout' of bird breeding sites. Impacts on lives and livelihoods include: overtopping and breaching of earthen embankments with extensive flooding of reclaimed marshes and loss of agricultural production; saltwater intrusion into coastal valleys; flooding

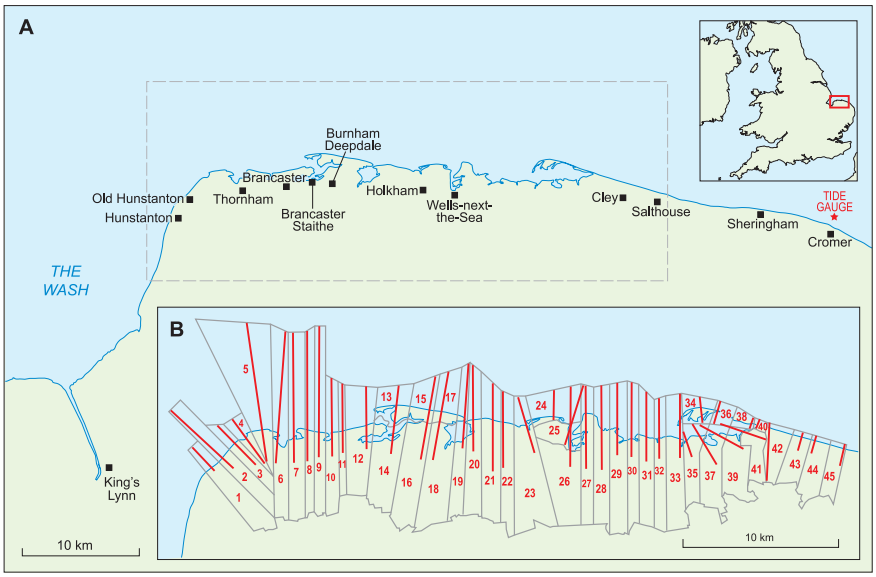

Figure 1: North Norfolk case study site, A) Location map, B) Regional coastal assessment sections and transects for hazard assessment

of coastal settlements with disruption to shops and businesses in larger settlements; disruption to inshore fisheries, local shellfish industry and, at Wells-next-the-Sea, port activities; and road flooding, including closure of the main W-E road network.

3. Identification of Coastal Risk Hotspots

Initially the risk hotspots from extreme events over the entire 45 km frontage were identified in a regional assessment. Risk is defined as the probability of a hazard, its extent, and its consequences. A probabilistic response approach was used, in which the probability of occurrence of the hazards was determined. We show below how the hazard extent was calculated by empirical formulae, based on the potential type of hazard experienced (Holman, 1986; Stockdon et al., 2006; Pullen et al., 2007; Donnelly, 2008). A coastal exposure indicator was used to calculate the relative risks experienced by different flooded areas; this was based on hazard severity, land use, population and social vulnerability,

transport systems, utilities and business settings (Viavattene et al., 2015).

The assessment framework required the region to be divided into representative sectors, to capture the spatial variability in the bathymetry/topography and extreme event forcing. A total of 45, 1-2 km wide sections (Figure 1) were generated, based on topographical features, location of towns, and type of ecosystem. For each section, a representative shore-normal transect was selected. On the UK east coast, the Environment Agency (EA) has undertaken long-term monitoring of coastline change through bi-annual shore-normal transect surveys, at an alongshore spacing of 1 km, since 1992. Where possible, the EA transects were chosen for this analysis.

Bathymetry data was drawn largely from the UK Hydrographic Office (UKHO) MEDIN bathymetry dataset, at resolutions ranging from 1 to 200 m. Near to the coast, 1 m resolution DTM LIDAR data (obtained from the EA) from January and February 2014 was used, with gaps in this data being filled with the 1 km EA shore-normal profile data described above. Further inland, topographical data was taken from 5 m resolution UK Ordnance Survey data (EDINA Digimap Ordnance Survey Service[1]). At the study site there is a datum shift between the bathymetry Chart Datum (CD) and the topographic Ordnance Datum Newlyn (ODN); this shift varies across the study site. In order to join the bathymetry and topography data together, the UKHO Vertical Offshore Reference Frame (VORF) surface (Lessnoff, 2008) was used.

3.1. Regional Hazards

The extent of the flooding was calculated with a probabilistic response method based on the type of hazard (wave runup, wave overwash, overtopping) experienced at each sector. A scale of storm hazard was used to determine the type of hazard experienced at each transect, relating the water level reached to the height of the first line of defence, i.e the crest of earthen embankment/seawall/dune. The scale of storm hazards was modified from Sallenger Jr

[1] https://www.digimap.edina.ac.uk

(2000), the modification is necessary as we were interested in the inundation over the intertidal zone (i.e. saltmarsh) which can occur when the first line of defence, often an earthen embankment, seawall or dune, is not exceeded. We therefore distinguished inundation landward of the first line of defence as terrestrial inundation. The modified impact classification regime is shown in Table 1.

In the swash regime the wave runup, defined as the height reached by the swash above the still water level (including wave setup), is confined to the foreshore. For the swash regime the hazard extent was calculated from the height of the total water level (tide+surge+wave runup). For the overwash and terrestrial inundation regimes, the hazard extent was taken as the overwash extent. As the topography is very varied within most of the sections, the overwash extent was adapted to follow the topographic contours on either side of the transect.

The hazard was assessed using a response approach for a 1 in 115 year return period storm. The 1 in 115 year return period was chosen as it is the return period for the recent extreme storm surge event in December 2013, as calculated by the method in Section 3.1.2. The December 2013 storm surge is the highest magnitude event in the last 60 years recorded on UK East coast tide gauges (Steers et al., 1979; Haigh et al., 2015; Spencer et al., 2015). During the event peak significant wave heights offshore from North Norfolk reached 3.8 m and reached 2.9 m inshore. Maximum surge residuals reached 1.97 m at Immingham tide gauge (90 km North East of the study site) and 2.18 m at Lowestoft tide gauge (70 km South West of the study site). The peak in storm surge residual closely preceded high water level (Spencer et al., 2015).

3.1.1. Water Level

A long water level record (tide+surge) was obtained from the tide gauge at Cromer (UK National Tidal and Sea Level Facility NTSLF[2]), 12 km east of the case study site. The Cromer gauge has records from 1973 to the present but

[2]https://www.ntslf.org

Swash Regime	$\frac{R_{high}}{D_{high}} < 1$	Runup confined to foreshore
Overwash Regime	$\frac{R_{high}}{D_{high}} > 1$ and $\frac{R_{low}}{D_{high}} < 1$	Runup exceeds the elevation of the first line of defence
Terrestrial Inundation Regime	$\frac{R_{high}}{D_{high}} > 1$ and $\frac{R_{low}}{D_{high}} > 1$	Elevation of the base of the swash motion exceeds the elevation of the first line of defence

Table 1: Coastal impact classification modified from Sallenger Jr (2000). Where R_{high} and R_{low} are the representative high and low water levels, and D_{high} and D_{low} are the high and low frontage elevations.

there are large gaps in the record. In particular, due to the gauge's location under Cromer pier, there are typically no maximum water level readings during large storm surges (e.g. 2013 storm surge). Hindcast modelled water level data (tide+surge) from the UK National Oceanography Centre (NOC) CS3X Continental Shelf tidal surge model (Flather, 2000) at the closest grid point to Cromer (19 km distance) was used to fill in some of the gaps during large storm surge events. Hindcast data was obtained for four weeks surrounding the largest storm surges for which data was available (12/12/1990, 20/02/1993, 10/01/1995, 19/02/1996, 14/12/2003, 31/10/2006, 17/03/2007, 08/11/2007 and 05/12/2013 storm surges (Brooks et al., 2016)). As the model data point is offshore in deeper water than the tide gauge, an empirical transformation function was determined between the modelled hindcast water level and the tide gauge water level. For the time periods where there is concurrent modelled and tide gauge data, the extreme sea levels were selected. Extreme values were defined as the water levels above the 95th percentile, occurring at least 3.5 days apart in order to separate individual storms. Haigh et al. (2015) found that the effect of storms which give rise to high water levels around the UK coastline typically last 3.5 days. The regression analysis found a good fit between the tide gauge and modelled data ($y = 0.951x + 0.478$, $R^2 = 0.864$). The transfer function was applied to the modelled water level data and combined with the tide gauge water level data, providing a record length of 25.4 years (Figure 2a).

There is a significant variation in tidal levels with distance along the North Norfolk coast (1.5 m difference in mean high water springs between Cromer and Hunstanton) due to variations in tidal range. The relationship between the height of mean high water springs (MHWS) water level from Admiralty tide tables (Environment Agency, 2010) and Easting (British National Grid) (Figure 2b) was fitted with a regression line of $y = 2.664x10^{-5}x + 18.514, R^2 = 0.938$. The fitted slope was used to calculate the difference in water level at each transect from the value at Cromer, based on where the transect crosses the shoreline.

3.1.2. Offshore wave climate and inshore wave transformation

A long (35.5 year) wave data series was obtained from the Met Office Wavewatch III (WWIII) model (Bunney and Saulter, 2015) at location $53.109N$ $0.615E$ (5 m water depth). For the period January 1980 to June 2015, waves were predominately from the North to North-East at this location. The mean significant wave height (H_s) over the period was 0.75 m, and the maximum significant wave height reached was 4.70 m.

The presence or absence of saltmarsh along a transect was assessed using an Environment Agency habitat map. For all transects with saltmarsh (23 out of 45 transects), the wave transformation over the vegetation was determined using a 1D SWAN model. SWAN is a third generation spectral wave model for computation of waves in shallow water (Booij et al., 1996). The 1D SWAN transects were set up with a 10 m resolution using the transect bathymetry and the location of the saltmarsh along the transect. The resolution allowed the variations in marsh topography to be represented in the grid. Wave dissipation was calculated along the transect from 5 m water depth to the landward limit of the saltmarsh using a modified SWAN vegetation module which better represents the dissipation due to vegetation under storm conditions (Roelvink et al., 2015).

To reduce the number of model runs, a set of representative wave data was created for each saltmarsh covered transect. The relationship between the

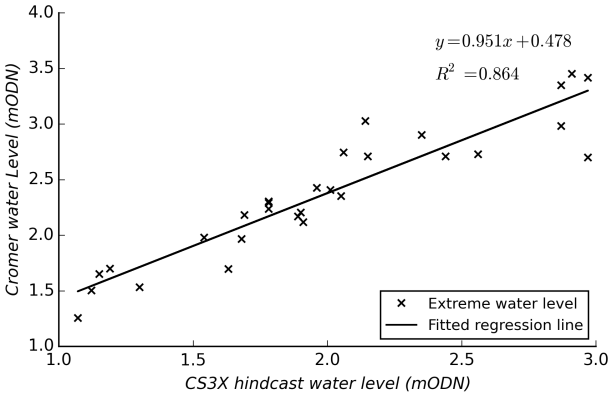

(a)

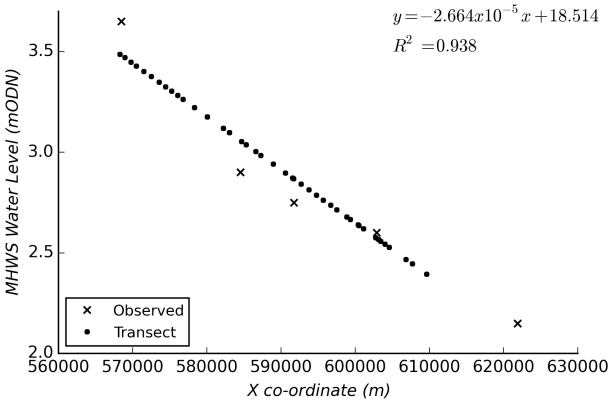

(b)

Figure 2: Regression analysis for (a) Transformation function between Cromer tide gauge and offshore modelled water levels, (b) Mean high water level and distance along the coast. mODN = m Ordnance Datum Newlyn where 0.0 m ODN approximates to mean sea level.

offshore significant wave height (at 5 m water depth) and water depth, or offshore relative wave height (H_s/h), was calculated at each of the transects over the full wave record. Water levels for three return periods (25, 100 and 115 years) were calculated for each transect to provide a range of potential water levels. The extreme water levels for each transect were determined with a peak over threshold analysis. Water level peaks above the 99.9th percentile and with a separation of 3.5 days between peaks were selected as the extreme values. The analysis identified 111 extreme water level events over the record length of 25.4 years, an average of 4.4 storms per year. These extreme water levels were fitted with a generalized pareto distribution and the resulting curve was extrapolated to determine storm return periods (Figure 3).

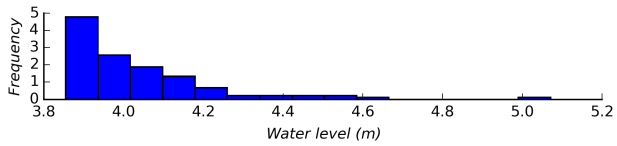

(a)

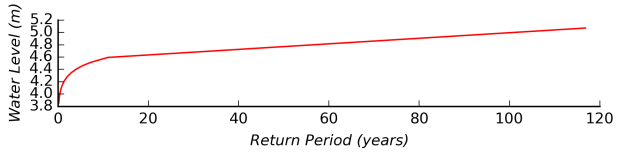

(b)

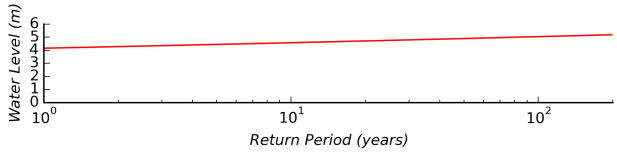

(c)

Figure 3: Extreme water level (m ODN) analysis for Transect 1. a) frequency distribution histogram for extreme water levels, fitted with a generalised pareto distribution; b) water level return period from the extreme water levels; c) extrapolated return period for water level.

The relative wave height was calculated and sorted and 8 percentiles were chosen based on the full range of data for each water level. The 8 wave conditions for each of the 3 water levels were then run through the SWAN model using stationary wave parameters and water depth, and the wave height reduction calculated. The relationship between the relative wave height and the wave height reduction was calculated using an ordinary-least squares regression for each transect (an example relationship for Transect 18 is presented in Figure 4, length of the saltmarsh for Transect 18 is 375 m). This wave height reduction formula was then applied to the full wave record for all the subsequent calculations.

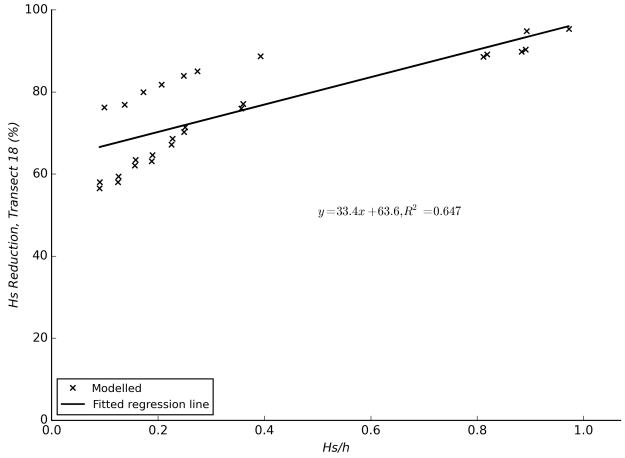

Figure 4: Relative wave height (H_s/h) and wave height dissipation due to the presence of saltmarsh vegetation at Transect 18 (saltmarsh length is 375 m)

3.2. Hazard Calculation

The probability of occurrence of the hazards was determined using a response approach. The hazard magnitude was calculated from the the full wave and tidal record and the probabilistic distribution of the hazard was used to produce a 1 in 115 year return period event. The calculations resulted in hazard extents and an index of hazard severity for each section.

3.2.1. Wave Runup

Wave runup was calculated for each of the 45 transects along the case study site. The transects were classified into those with a natural beach slope (31 transects) and those with a man-made artificial frontage (14 transects). For the natural beach slope transects, the wave runup was calculated over the full wave records according to Stockdon et al. (2006) and Holman (1986).

Runup in Stockdon et al. (2006) is predicted as:

$$Ru_{2\%} = 1.1\left(0.35\tan\beta\left(H_sLo\right)^{1/2} + \frac{\left(H_sLo\left(0.563\tan\beta^2 + 0.004\right)\right)^{1/2}}{2}\right) \quad (1)$$

under dissipative conditions ($\zeta < 0.3$):

$$Ru_{2\%} = 0.043\left(H_sLo\right)^{1/2} \quad (2)$$

where H_s is the significant wave height, Lo is the wave length, $\tan\beta$ is the beach face slope defined as the beach slope where the predicted water level intersects the beach, and ζ is the Iribarren number, defined as:

$$\zeta = \frac{tan\beta}{\sqrt{\frac{H_s}{Lo}}} \quad (3)$$

Runup in Holman (1986) is predicted as:

$$Ru_{2\%} = H_s\left(0.83\zeta + 0.2\right) \quad (4)$$

The runup calculated from each method was added to the water level at each transect and then compared with high resolution (three dimensional coordinate quality $<$ 50 millimetres and typically $<$ 20 millimetres) Real Time Kinetic (RTK) measurements taken on or behind shoreline features immediately after the December 2013 storm surge. The Stockdon et al. (2006) method gave the best results for gravel and sand beaches whereas the Holman (1986) equation gave the best predicted total water level for transects with saltmarsh.

For the artificial beach transects, the wave runup was calculated using the EurOtop method (Pullen et al., 2007). For each transect, the surface roughness

at the beach slope was estimated on the basis of the flood defence material characteristics.

The wave runup for the 115 year return period used the same probabilistic method as had been used to calculate the extreme water level values: a peak over threshold analysis was used to select the extreme values; the extreme wave runup threshold was taken as the 99.5th percentile; and extremes were only detected if separated by a minimum of 3.5 days. This analysis generated 155 extreme events at an average of 4.4 events per year. The extreme values were fitted with a generalized pareto distribution and the return period was determined.

For transects and storms within the swash regime the total water level (tide+surge+wave runup) was calculated and a contour at the total water level used to demarcate the hazard extent for each sector.

3.2.2. Wave Overwash

For transects and storms within the overwash or terrestrial inundation regime (where the water level exceeded the first line of defence) the wave overwash depth (h_c) was calculated using the method of Donnelly (2008).

$$h_c = \frac{h_0}{x_R}\left(x_R - x_C\right) \tag{5}$$

where h_0 is the depth at the still water line during maximum runup, x_C is the difference between the still water level and the maximum beach height, x_R is the horizontal projection of maximum runup from the still water level. The term $\frac{h_0}{x_R}$ can be substituted by a constant value based on empirical data by Schüttrumpf and Oumeraci (2005):

$$\tan\beta \geq 0.21, \frac{h_0}{x_R} = 0.028 \tag{6}$$

$$\tan\beta < 0.21, \frac{h_0}{x_R} = 0.035 \tag{7}$$

The coefficient x_C was measured directly from the transect bathymetry, the coefficient x_R was calculated as wave runup divided by the beach slope. To account for volume of water lost due to infiltration the evolution of h_c was

calculated as:

$$h(x) = h_c e^{-a\frac{x}{u_c}} \tag{8}$$

where a is the proportionality constant for infiltration ($a = 0.01$ for an impermeable bed, else $a = 0.12$), u_c is the flow velocity at the highest point of the beach:

$$u_c = C_u\sqrt{gh_c} \tag{9}$$

where C_u is the bore front coefficient ($C_u = 1.53$ for a sandy beach (Donnelly, 2008), $C_u = 2$ for a man-made frontage (analytical dam break solution), and $C_u = 2.6$ for a gravel barrier (Matias et al., 2014)).

The hazard extent was determined as the maximum distance at which the overwash depth was greater than 0.01 m.

3.3. Regional hotspots of risk

A coastal index for flooding, resulting from variations in the severity of the hazard experienced and a range of vulnerability measures, was developed by Viavattene et al. (2015). It was used to compare the different sectors along the North Norfolk coast and identify risk hotspots:

$$CI = (i_h \times i_{exp})^{\frac{1}{2}} \tag{10}$$

where i_h is the hazard index and i_{exp} is the overall exposure indicator defined as:

$$i_{exp} = (i_{LU} \times i_{POP} \times i_{TS} \times i_{UT} \times i_{BS})^{\frac{1}{5}} \tag{11}$$

where i_{LU} is the exposure indicator for land use, i_{POP} is the indicator for population and social vulnerability, i_{TS} is the indicator for transport systems, i_{UT} is the indicator for utilities, and i_{BS} is the indicator for business settings.

3.3.1. Flooding Hazard Index

In this research, the flooding hazard index was calculated in two ways, depending upon the flooding regime present. For transects in the swash regime, the hazard value was determined from the mean water depth over that part of

the transect above the mean high waterline. For transects in the overwash or terrestrial inundation regime, the hazard value was determined from the overwash depth immediately behind the coastal defence. The hazard index values were assigned to the water depths using Jenks Natural Breaks classification (Jenks, 1967) based on the range of results (Table 2).

Hazard Index	Runup Mean water depth (m)	Overwash Water depth (m)
0	0	0
1	0.01 - 1.51	0.01 - 0.27
2	1.51 - 1.84	0.27 - 0.44
3	1.84 - 2.49	0.44 - 0.96
4	2.49 - 3.65	0.96 - 1.43
5	3.65 - 5.14	1.43 - 2.27

Table 2: Hazard Index based on the type of coastline and calculation method

3.3.2. Exposure Indicator: Land Use

The land use exposure indicator (i_{LU}) is determined by:

$$i_{LU} = \sum_{j=0}^{n} S_j \times V_j \tag{12}$$

where n is number of land use classes, S is the normalised surface area, and V is the importance value.

The distribution of land use types within the North Norfolk case study site was obtained from Land Cover data from 2007, accessed through EDINA Digimap[3]. Importance values were assigned to each land use class based on expert knowledge and perceived importance within the study area. The highest importance values were assigned to built-up areas (suburban, urban or industrial). Some natural habitats were assigned high values, such as fen marsh and swamp, as these attract the wild birds that bring many of the tourists to the area, generating income and livelihoods.

[3]https://www.digimap.edina.ac.uk

3.3.3. Exposure Indicator: Population and Social Vulnerability

The population and social vulnerability exposure indicator (i_{POP}) was calculated based on the Social Flood Vulnerability Index (SFVI) for census areas in England (Tapsell et al., 2002). The SFVI is a composite additive index based on four characteristics: financial deprivation (unemployment, overcrowding, non-car ownership and non-home ownership); age; household structure; and health. Data for the four characteristics was transformed into percentages based on the total population of the census areas. The $SFVI$ was calculated as:

$$SFVI = SFVI_s + SFVI_p + SFVI_e + \frac{1}{4}\left(SFVI_u + SFVI_o + SFVI_c + SFVI_h\right) \tag{13}$$

where $SFVI_s$ is the SFVI indicator for long-term sick, $SFVI_p$ is the SFVI indicator for single parents, $SFVI_e$ is indicator for the elderly, $SFVI_u$ is the indicator for unemployment, $SFVI_o$ is the indicator for overcrowding of households, $SFVI_c$ is the indicator for non-car ownership, and $SFVI_h$ is the indicator for non-home ownership.

SFVI was calculated for each census area and the values split into five categories, using the Jenks Natural Breaks classification method. The categories of SFVI were then assigned i_{POP} values in Table 3.

Category	SFVI value	i_{POP}
Very low vulnerability	-1.19 to -0.72	1
Low vulnerability	-0.72 to -0.03	2
Medium vulnerability	-0.03 to 0.38	3
High vulnerability	0.38 to 1.83	4
Very high vulnerability	1.83 to 2.78	5

Table 3: Population and social vulnerability indicator values

3.3.4. Exposure Indicator: Transport Systems

The transport systems indicator i_{TS} was calculated based on the type and importance of the transport system flooded. The exposure indicator value categories are presented in Table 4. The transport system within the case study

site were limited to roads only, with the key road being the A149 from Kings Lynn (to the West) to Cromer/Sheringham (East). Flooded sectors with highest category A roads were given $i_{TS} = 3$, B roads $i_{TS} = 2$, and sectors with no A or B roads $i_{TS} = 1$.

Category	i_{TS}
No significant transport network within flood extent	1
Mainly local and small network within flood extent	2
Presence of transport network with local/regional importance	3
High density and multiple networks (train, road, airport) of local importance or regional importance	4
High density and multiple networks (train, road, airport) of national or international importance	5

Table 4: Transport system exposure indicator values

3.3.5. Exposure Indicator: Utilities

The utilities indicator i_{UT} was calculated based on the density and importance of utility assets or networks (Table 5). Utilities data for this stretch of coast were collected from on OpenStreet maps and a site inspection. Point data was obtained for water pumping stations, sewage treatment plants, electricity sub-stations, mobile phone masts and emergency services. Most of the sectors have no utilities or utilities of only local importance ($i_{UT} = 1$ or 2). The life boat station at Wells-next-the-Sea gave this location an index value of 3.

Category	i_{UT}
No significant utility network/asset within flood extent	1
Utility of local importance	2
Medium density or multiple utility network/asset of local importance	3
High density and multiple utility networks/assets of regional importance	4
High density and multiple utility networks/assets of national importance	5

Table 5: Utilities exposure indicator values

3.3.6. Exposure Indicator: Business Settings

The importance of commercial properties within the flood extents was checked by visual inspection and then used to calculate a Business Settings exposure index (i_{BS}). The index was determined using the ranking in Table 6 with the maximum exposure index within each flooded section being selected. Business setting index values of 2 were given to businesses with a local importance only and include general stores, hairdressers and boat storage. Index values of 3 were given to businesses with a greater importance in the local economy. They included tourist shops, cafés, restaurants and public houses. Business index values of 4 were given to larger pubs and restaurants, as well as camping and caravan sites, Bed and Breakfast (B&B) establishments and hotels. Businesses deemed to have a national importance and hence given an index value of 5, include the Royal West Norfolk Golf Club, the Wells outer harbour which services the Sheringham Shoal offshore wind farm, and the Blakeney Hotel.

Category	i_{BS}
No significant economic activities	1
Mainly local small economic activities	2
Local/Regional economic activities	3
Economic activities with regional importance	4
Economic activities with National or International importance	5

Table 6: Business settings exposure indicator values

3.4. Results and Hotspot Selection

Results of the CRAF Phase 1 assessment are presented in Figure 5. The Coastal Index values ranged between 1.00 and 3.57, with a mean value of 2.06. The coastal index (Figure 5g) highlighted hotspots at Old Hunstanton, Thornham, Titchwell Nature Reserve, Brancaster/Brancaster Staithe/Burnham Deepdale, Burnham Overy Staithe, Holkham, Wells-next-the-Sea, and Salthouse. The hotspots are generally located in sectors with residential to urban elements.

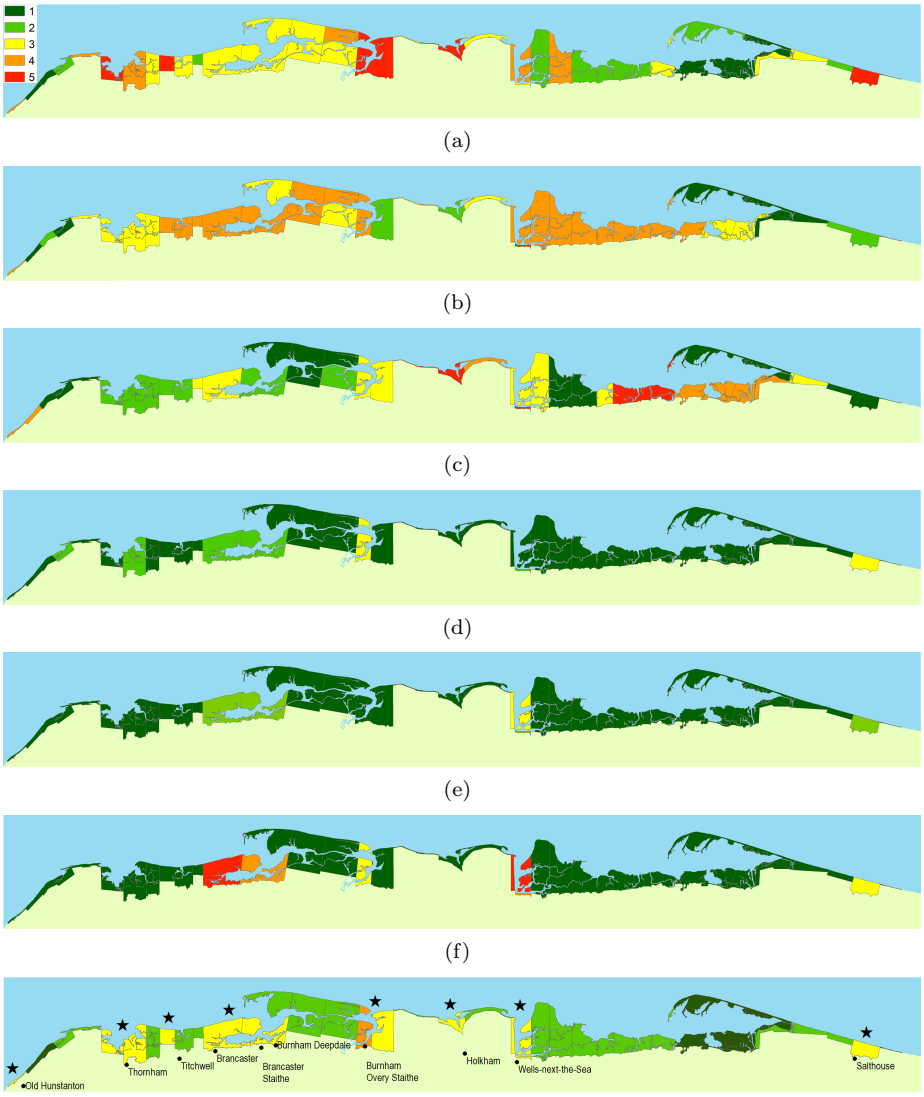

Figure 5: Exposure Indicators and Coastal Index; a) Hazard indicator, b) Land Use exposure indicator, c) Population and social vulnerability exposure indicator, d) Transport system exposure indicator, e) Utilities exposure indicator, f) Business exposure indicator, g) Coastal Index. Hotspots are identified with stars.

4. Comparison of Hotspots

Two hotspots were selected for further modelling and comparison in CRAF Phase 2, Brancaster/Brancaster Staithe/Burnham Deepdale and Wells-next-the-Sea. These two hotspots represented two of the three highest coastal indices generated by Phase 1 (CI =3.36 and 3.00 for Wells-next-the-Sea and Brancaster, respectively). Additionally they showed a variety of topographic/bathymetric features and receptor data in order to test the Phase 2 method. CRAF Phase 2 used more complex and higher resolution hazard and vulnerability modelling methods than CRAF Phase 1. Hazards were calculated using 1D process based XBeach model transects (Roelvink et al., 2010), and a LISFLOOD-ACC inundation model (Bates et al., 2013). XBeach is a coupled flow, wave and sediment transport model for simulation of nearshore processes. XBeach was particularly suited to this research as it was originally designed to study nearshore response to extreme events, particularly overwash, dune erosion and breaching (Roelvink et al., 2009; McCall et al., 2010). LISFLOOD is an hydrodynamic inundation model designed for fluvial and coastal use. The LISFLOOD acceleration module (LISFLOOD-ACC) was used in this study, which solves the inertial formulation of the shallow water equations (Bates et al., 2010).The combination of the XBeach and LISFLOOD models allowed the inundation extent, water depth and flow velocity to be mapped in 2D. The combined models have been shown to be suitable for inundation modelling of storms by Prime et al. (2016), and they represent a significant saving in computational time from modelling inundation in a 2D XBeach inundation model.

Vulnerability to the hazards was calculated with the Integrated Disruption Assessment (INDRA) model (Viavattene et al., 2016). INDRA is an innovative open-access model which allows the assessment of direct and indirect impacts from an extreme coastal event. Standardised indicators come from a Multi Criteria Analysis.

The hazards were initially assessed at the two hotspots locations. The hazard information generated was then used as input data for the INDRA model.

Finally, an MCA was used to compare the regional impact at the two hotspots.

4.1. Local Hazard Assessment

The hazards were calculated in Phase 2 using an event approach for the December 2013 storm surge (1 in 115 year return period based on tide+surge). Hazard impacts at the two hotspots were assessed through the generation of multiple transects for each hotspot (41 transects at Brancaster (Figure 6a), 58 transects at Wells (Figure 6b)). Transects were selected based on the variation in topography of the first line of defence. The transects were perpendicular to the shoreline except in the embankment running North-South at the Wells harbour where transects followed the lines of channels. XBeach modelling at each transect was driven by water level and wave conditions for the December 2013 storm event. Wave conditions were input as a JONSWAP spectra generated in XBeach from the storm wave parameters. XBeach was run with no morphological updating, as it was considered that erosion would not impact the vulnerability indicators at these locations.

Water level data was obtained by the same method as CRAF Phase 1 (see Section 3.1.1). The wave data record was obtained from the Met Office WWIII model at 2 locations, 53.109N 0.615E for Brancaster and 53.102N 0.882E for Wells.

The XBeach model was run with the default parameters, unless otherwise stated. Energy dissipation due to vegetation was included in the modelling for those transects containing saltmarsh. Vegetation height was taken as $H_v = 0.11$ m (field data from Stiffkey, North Norfolk (Möller et al., 1999)), plant diameter as $D_v = 0.00125$ m (Möller et al., 2014), and plant density ($stems/m^2$) as $N_v = 1061$ (field data for comparable saltmarsh communities at Tillingham, Essex (Möller, 2006)).

The spatially variable overtopping discharge generated by the XBeach modelling was used as input conditions for the LISFLOOD inundation model at the two hotspots. The discharge was applied 1 m beyond the first line of defence with a 30 minute frequency. Due to the complex bathymetry with

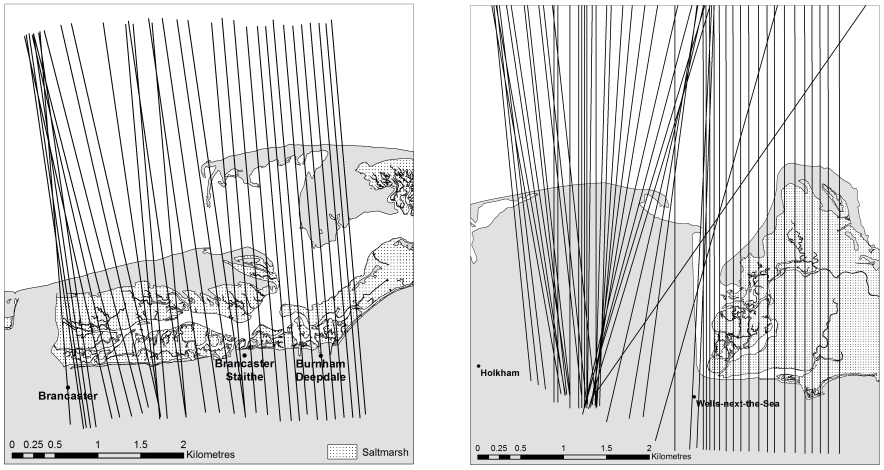

(a) (b)

Figure 6: XBeach transect locations for assessment of hazards in risk hotspots for (a) Brancaster/Brancaster Staithe/Burnham Deepdale and (b) Wells-next-the-Sea

creeks/channels/barrier islands the transect method fails to fully represent the hazard, as it cannot represent all flow pathways. Therefore, the time-varying tidal water level for the event was used as an input to the LISFLOOD model together with the discharge. The tidal water level was defined at a frequency of 30 minutes over a grid of 200 x 200 m resolution to properly represent flooding of the complex bathymetry.

The LISFLOOD model used bathymetry/topography resampled onto a 5x5 m grid (See Section 3). The Wells grid DTM was updated to include the heights of the town's flood wall and demountable barrier. For both hotspots, a Mannings coefficient of 0.06 (land use of dense grass) was used and an infiltration rate of $1 \times 10^{-7} ms^{-1}$ (British Geological Survey (BGS) superficial permeability indices from EDINA Digimap and Brouwer et al. (1988)).

The inundation modelling produced maximum water level and maximum depth-velocity product (maximum of the water depth $\times$ the depth-averaged velocity at each grid cell over the computation period) across the hotspots. Additionally wave heights across the transect were extrapolated over the salt-

marsh, and the duration of the flood event over freshwater grazing marsh was determined (assuming an infiltration rate of 7.5 mm/hr).

4.2. Regional Impacts

The impacts of the two selected hotspots in a regional context was assessed with the INDRA model. The overall impact score is based on the aggregation of 8 impact indicators: risk to life; household displacement; household financial recovery; business supply chain disruption; business financial recovery; impacts to ecosystems and agriculture; and disruption to transport networks (Viavattene et al., 2015). In INDRA, impacts are both direct, in response to the exposure of a receptor, and indirect, occurring outside the flooded area and/or continuing after the food event.

4.2.1. Direct Impacts

All residential and commercial properties were identified with the UK Environment Agency's National Receptor Dataset (NRD), a database of the type, size and location of land use which could be impacted by a hazard. For each of the property types, flood damage thresholds were determined using susceptibility curves obtained from Penning-Rowsell et al. (2016). All residential properties were assigned an average set of thresholds. Individual thresholds were developed for shops, hotels, catering establishments, caravans, B&B establishments and holiday cottages. Building collapse thresholds, based on the depth-velocity product, were taken from Karvonen et al. (2000).

The ecosystem considered to be important for this case study site are crops (in particular winter cereals, selected as most flood events occur during the winter months), freshwater grazing marsh and saltmarsh (Table 7). The 2007 Land Cover data from EDINA Digimap was used to identify the location of these types of land cover. The areas were then resampled and converted to point data with a 15 m resolution.

Risk to Life was measured using the method of Priest et al. (2007), based on the depth-velocity product and the vulnerability of the receptor (Table 8).

	Wave Height (m)				
Depth (m)	<0.3	0.3-0.6	0.6-1	1-2	>2
0 to 1	0	2	2	3	3
1 to 2	0	1	2	2	3
2 to 3	0	1	1	2	2
3 to 4	0	0	1	1	2

0: No effect
1: Changes within normal seasonal variation
2: Changes beyond normal seasonal variation, but partial/total recovery
3: Irreversible change

Table 7: Saltmarsh Ecosystem Vulnerability Indicator

Vulnerability of the area was defined based on the land use data from the NRD and scored on a scale of 1-3. Point data for each receptor is assigned at one of the three levels: low vulnerability applies to multi-storey apartments, masonry concrete and brick properties; medium vulnerability applies to typical residential areas with mixed type of properties; and high vulnerability applies to mobile homes, camp sites, bungalows, and poorly constructed properties. The NRD does not supply information on property construction for residential properties, therefore they are assumed to be of mixed type with medium vulnerability. The area vulnerability was calculated by aggregating and normalising the individual exposed receptors vulnerability score. The depth-velocity product was then used to determine the level of risk to life, from low to very high risk.

	Nature of the Area		
Depth-velocity product m^2s^{-1}	Low Vulnerability	Medium Vulnerability	High vulnerability
<0.25	Low risk	Low risk	Low risk
0.25-0.50	Low risk	Medium risk	Medium risk
0.50-1.10	Medium risk	Medium risk	High risk
1.10-7	Medium risk	High risk	Very High risk
>7	Very High risk	Very High risk	Very High risk

Table 8: Risk to Life matrix

4.2.2. Displacement and reinstatement time

An indirect impact on households and businesses was assessed through the displacement time and reinstatement time, linked to the low, medium, high and very high thresholds of direct impacts for each receptor.

For household displacement, a dataset was analysed containing 5000 UK insurance claims, collected and supplied by WeatherNet[4]. This provided information on the total claim per property and the associated cost of alternative accommodation. Using UK depth-damage curves, and an average cost per displacement event taken from Penning-Rowsell et al. (2016), it was possible to ascertain the likely duration of displacement and the likely flood depth inside each property. With this information, the percentage of households displaced due to the direct impacts considered was calculated (Table 9).

Specific data on business recovery time in relation to flood depth is very limited. Using media reports and grey literature, reinstatement times for hotels, catering establishments and shops in North Norfolk were set at 182, 105 and 30 days for high, medium and low threshold events respectively. The equivalent reinstatement times for Bed & Breakfasts and holiday cottages were set at 225, 105 and 30 days. Static caravans were considered to be a total loss once infiltrated by floodwaters (Penning-Rowsell et al., 2013); it was assumed that it takes 4 months to replace these assets.

4.2.3. Financial Recovery

The financial recovery was assessed with a matrix relating thresholds of direct impact on a property and the type of financial recovery mechanism(s) (insurance, savings etc.) present. Information on the percentage of insured and non-insured households by income decile was derived from datasets held by the Office for National Statistics (ONS) (2014). These percentages were then linked to average weekly income. The results showed little variability across the case study area, with slightly higher levels of prosperity to the west. These

[4]http://www.weathernet.co.uk

		Direct Impact on Property			
	Index	Low	Medium	High	Very High
Not displaced	0	0.87	0.30	0.18	n/a
Displaced for up to 1 month	1	0.03	0.04	0.01	n/a
Short term displacement, > 1 month <= 3 months	2	0.05	0.17	0.07	n/a
Medium term displacement,>3 month <=12 months	3	0.05	0.40	0.49	n/a
Long lasting displacement, > 12 months	4	0	0.09	0.25	n/a
Never return to the original property	5	0	0	0	n/a
Total Receptor Distribution		0.28	1.94	2.62	n/a

Table 9: Household displacement matrix

insurance penetration figures were adjusted to take into account the estimated 20% (Association of British Insurers (ABI), undated a) of under insured UK households. The likely percentage of self-insured households was also assessed. Self-insurance is defined as those households which have sufficient savings to cover the cost of damages to property and contents, based on the average cost of flood insurance claims (ABI, 2016) and household savings in the UK (Scottish Widows, 2014).

Around 95% of UK businesses are insured for buildings, contents and/or disruption. Again, this figure was reduced to take into account data on under insurance (ABI, 2007; AXA, 2007) and the potential for small business to recover without external assistance (ABI, undated b). All the North Norfolk businesses in potentially impacted areas are small or micro-sized business (i.e. likely to have fewer than 10 employees) and are typically independent shops, cafés or restaurants.

4.2.4. Transport Disruption

The systemic impacts were determined in INDRA through a network analysis technique, which defines the network as a series of nodes and the links between them. The transport disruption was assessed through a Weighted Dis-

connection and Time Lengthening (WDTL) indicator developed by Viavattene et al. (2015). This indicator is the product of the ratio of the time taken for a journey before and after a flood event and the ratio of connectivity before and after a flood event. To calculate the connectivity ratio the nodes are weighted by their importance. The INDRA model required a map of the transport network with links (roads) and nodes (junctions), speed limits across the network, an importance value for the junction and a reinstatement time

A shapefile of the regional road network was produced in ArcGIS based on a geographically-referenced layer taken from Ordnance Survey (OS) Mastermap. The expected maximum speed of vehicular traffic was assigned using a combination of Google Street View[5] and national speed limits. A value between 1 (no importance) to 10 (very high importance) was assigned to each of the 38 junctions in the road network. This was based partly on daily traffic flow data, available for various sections of the A149 (Department for Transport, 2016) with the location of emergency assets also being taken into consideration. Based on information from past local flood events, it was assumed that roads will be impassable for up to 4 days following a flood event to allow for the removal of sediments and other debris; recent major surges have been accompanied by the deposition of extensive rafts of vegetation debris, stripped by storm water levels and waves from saltmarshes and reedbeds, onto road surfaces (Spencer et al., 2015). If major storms are accompanied by high rainfall, and arable field cover on the high ground to the south of the A149 is seasonally low, then 'muddy floods' (Boardman et al., 2003) can deposit layers of sands, silts and muds on roads and within coastal villages.

4.2.5. Business Disruption

The systemic impact of business disruption was also calculated through a network analysis. The disruption to business was assessed through a business supply chain framework which characterises the supply and demand. Businesses

[5]https://www.google.co.uk/maps

and supply sources were mapped as nodes and the conveyance of goods/services mapped as a link. An overall business disruption indicator was calculated as the sum of the reduction in supply capacity of nodes weighted by their importance to the local economy (Viavattene et al., 2015). The regional supply chains were simplified to focus on the main industry.

Due to the importance of tourism to the Norfolk economy, the tourism industry was selected for the business supply chain analysis. Tourism is the largest economic sector in the county of Norfolk, valued at £2.96 billion in 2014, and accounts for around 17% of all regional employment (Destination Research, 2014). Annual visitor numbers are estimated at 571,000 for staying visitors (spending one night or more) and 5,948,000 day visitors (The South West Research Company, 2014). It was estimated that half of the above visit and stay near the coast in the case study region. Visitor numbers were adjusted to represent a typical day in the low tourist season (December) and high season (August). These numbers were then distributed along the coast, based on the number of attractions and availability of accommodation. Data is available (Royal Society for the Protection of Birds (RSPB), 2000) on the likely change in visitor numbers following damage or destruction to the receptors responsible for attracting visitors, principally bird habitats and birdwatching infrastructure and access to it, beaches, walking routes and accommodation. As a result of a change in visitor numbers, it is then possible to model the second-tier impacts on catering establishments, shops and accommodation. A schematic diagram of this business supply chain is provided in Figure 7.

4.3. Hotspot Comparison: Result of the Multi Criteria Analysis (MCA)

The weighting of the 8 impact indicators for the multi-criteria analysis are presented in Table 10. The weightings were selected using three different approaches:

- Method A uses a neutral approach, where each category is given equal weighting;

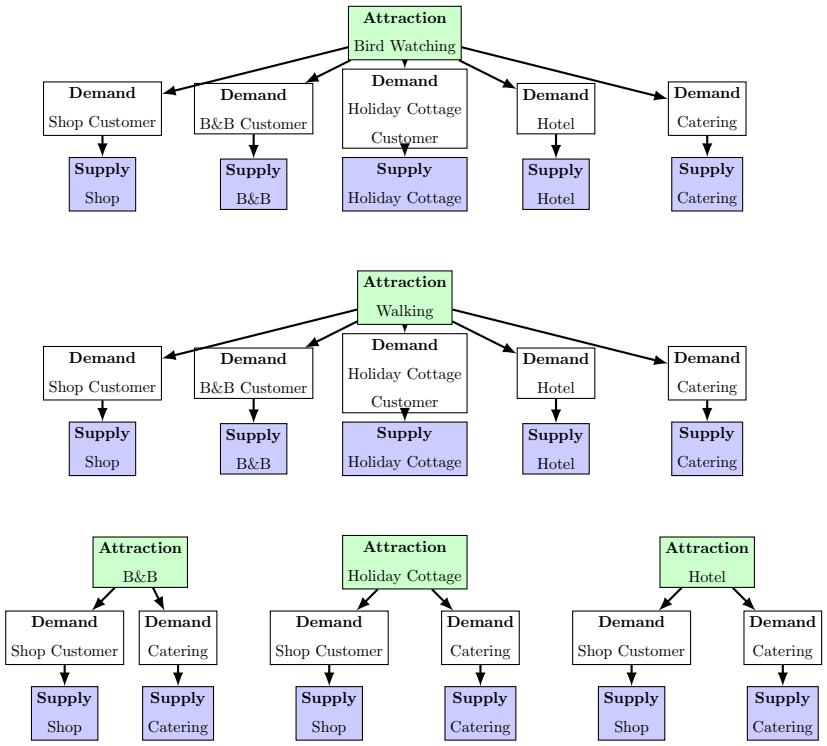

Figure 7: Schematic diagram of the business supply chain model. Showing attraction, demand, and supply nodes, and the relationship between natural activities (birdwatching and walking) and accommodation/catering facilities.

- Method B uses expert judgement where the importance of people, households and business are highlighted;
- Method C uses expert judgement where the importance of people and ecosystems are highlighted.

The hazard scenario for the 115 year return period flood event was used as input to the INDRA model. The model was run with a model simulation duration of 105 days for all three approaches. The simulation duration covered the reinstatement time for businesses from a medium impact event, which was the highest threshold reached for businesses.

The scores for the impact indicator categories for hotspots are presented in Table 11. For both hotspots, the business financial recovery was low and

business disruption only occurred in Wells. This low level of business disruption is most likely due to the spare capacity in the network at the hotspots. The transport system in Brancaster experiences no disruption for this magnitude of storm event, whilst in Wells there is a small transport disruption. The risk to life, household displacement and household financial recovery is higher at the Wells hotspot than at Brancaster. However, at Brancaster the ecosystems are more impacted than at Wells, for both managed (agriculture) and wetland ecosystems.

Category		**Weighting**		
		A	**B**	**C**
Population	Risk to Life	12.5	30	35
	Household Financial Recovery	12.5	10	5
	Household Displacement	12.5	15	5
Business	Business Financial Recovery	12.5	15	5
	Business Disruption	12.5	10	5
Ecosystem	Natural Ecosystem	12.5	5	20
	Agriculture	12.5	5	5
Transport	Transport Disruption	12.5	10	20

Table 10: MCA Weighting of the impact indicators using three approaches. A: a neutral approach, B: expert judgement with a household and business focus, C: expert judgement with an ecosystem focus.

The final MCA scores for the Wells and Brancaster hotspot sites are presented in Figure 8. The MCA scores for both hotspots sites are low, suggesting low impact from the flooding event. For the weighting methods A and C, the hotspot of Brancaster has a greater MCA score than the Wells hotspot, suggesting Brancaster experiences greater risk. This result is largely due to the high ecosystem indicator score at Brancaster, which both method A and C weight highly. For weighting method B, where ecosystems are weighted at a low level, Wells has a greater risk.

MCA Indicator Scores	Wells	Brancaster
Risk to Life	0.00083	0.00009
Household Financial Recovery	0.00014	0.00008
Household Displacement	0.00013	0.00011
Business Financial Recovery	0.00091	0
Business Disruption	0.00225	0
Natural Ecosystems	0.00316	0.01364
Agriculture	0.00003	0.00112
Transport Disruption	0.00249	0

Table 11: Multi Criteria Analysis vulnerability indicator score

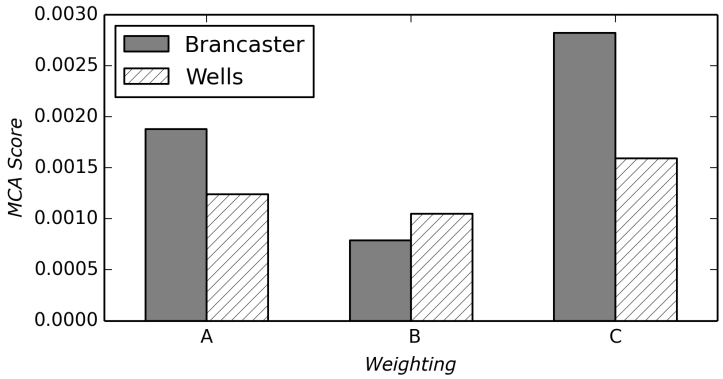

Figure 8: Total Multi Criteria Analysis Score

5. Discussion and Conclusions

New methods have been developed to initially identify parts of the coast at risk from high total water levels resulting from storm surge flooding, coastal 'hotspots', and then to prioritize the areas of risk identified. Working with coastal sections typically 1-2 km in width, variations in the extent of flooding alongshore were calculated from long term historical hydrodynamic conditions with empirical formulae. The modification to the hazard by natural coastal defences, such as saltmarshes, was also assessed. A probabilistic method was used to calculate the hazard based on the type of hazard experienced (wave runup, wave overwash, overtopping). A coastal indicator was used to calculate the relative risks experienced by different sections; this was based on hazard severity,

land use, population and social vulnerability, transport systems, utilities and business settings.

For the North Norfolk coast, 8 initial hotspots of coastal risk were identified. These hotpsots were then reduced to two locations for more detailed analysis. At this second stage, hazards were calculated using the 1D process based XBeach model for a series of closely spaced transects and a 2D LISFLOOD inundation model. Hazard outputs (for the 1 in 115 year return period event run over 105 days) were then input, alongside detailed information on the vulnerability to these hazards, into the INDRA model. Impact was calculated through both direct and indirect vulnerability indicators using a MCA approach. The vulnerability indicators were weighted to produce a final MCA score by expert judgement, this allowed perceptions of importance to be included in the analysis. In general, the analysis showed that business disruption and transport disruption from storm surge events impacting the North Norfolk coast is low, due to sufficient spare capacity within both these networks to absorb local shocks. Risks to life, household displacement and household financial recovery are also generally low, but greater in the hotspot which is a small town (Wells-next-the-Sea) than that formed of a chain of small villages (Brancaster / Brancaster Staithe / Burnham Deepdale). However, it is clear from the MCA analysis that the prioritization of resources for disaster risk reduction does depend on how different sectors are perceived as being of importance. If people, households and business are seen as being of greatest importance then small towns are likely to demand the greatest resources. However, if ecosystem valuation is included in the analysis (which may be of significance to coastal economies with a high dependency on income from nature-based tourism) then non urban settings can obtain much greater significance.

The CRAF tool has been shown to identify hotspots of risk through an initial screening followed by a comparison of the hotspots through a standardised assessment technique. The framework is resource efficient, using a hierarchical system which increases in both model complexity and spatial resolution for the smaller area hotspot comparison. It allowed focus on the key local economic

sectors, bringing together receptor vulnerability data from multiple sources to establish direct and indirect impacts. Furthermore, the staged analysis made the approach readily transferable to other coastal locations.

The transect approach used in both Phase 1 and 2 has the potential to lead to inaccurate hazard calculation as not all flow pathways are represented. In Phase 1, this was minimised by selecting sections based on similar topography and first lines of defence. In Phase 2 the tidal water level was input into the flood model to create a more realistic flow pattern, as such it was capable of replicating the complex coastal system. The study site is a relatively data rich coastline, which gives a high degree of confidence in the quality of the data. However, in some cases proxy data needed to be used where data was not available. Further applications along shorelines with different levels of data availability would usefully establish the minimum data requirement for the risk analysis.

Acknowledgements

This work was supported by the European Community's 7th Framework Programme through the grant to RISC-KIT ("Resilience-increasing Strategies for Coasts Toolkit"), contract no. 603458, and by contributions by the partner institutes and a grant from The Isaac Newton Trust, Trinity College, Cambridge. We would like to thank two anonymous reviewers for their comments and help improving the paper.

References

ABI, 2007. Summer floods 2007: learning the lessons, november 2007. Accessed 03 October 2016.
URL www.ambiental.co.uk/downloads/ABI_2007_Summer_Floods_Review.pdf

ABI, 2016. News release: New figures reveal scale of insurance response after recent floods, 11 january 2016. Accessed 03 October 2016.

URL https://www.abi.org.uk/News/News-releases/2016/01/New-figures-reveal-scale-of-insurance-response-after-recent-floods

ABI, undated b. Insurance for small businesses: a guide to protecting your business. Accessed 10 May 2017.
URL https://www.abi.org.uk/globalassets/sitecore/files/documents/publications/public/migrated/liability/insurance-for-small-businesses-a-guide-to-protecting-your-business.pdf

Abuodha, P. A., Woodroffe, C. D., 2006. Assessing vulnerability of coasts to climate change: a review of approaches and their application to the australian coast. University of Wollongon, Faculty of Science Papers.

Armaroli, C., Ciavola, P., Perini, L., Calabrese, L., Lorito, S., Valentini, A., Masina, M., 2012. Critical storm thresholds for significant morphological changes and damage along the emilia-romagna coastline, italy. Geomorphology 143, 34–51.

Association of British Insurers (ABI), undated a. Is your home underinsured? a guide to buildings and contents insurance. Accessed 03 October 2016.
URL https://www.abi.org.uk/~/media/Files/Documents/Publications/Public/Migrated/Home/Is%20your%20home%20underinsured.pdf

AXA, 2007. Preparing for climate change: A practical guide for small businesses. Accessed 03 October 2016.
URL http://nationalfloodforum.org.uk/wp-content/uploads/AXA-preparing-for-climate-change.pdf

Balica, S., Wright, N. G., van der Meulen, F., 2012. A flood vulnerability index for coastal cities and its use in assessing climate change impacts. Natural Hazards 64 (1), 73–105.

Bates, P., Trigg, M., Neal, J., Dabrowa, A., 2013. Lisflood-fp: User manual. University of Bristol, UK.

Bates, P. D., Horritt, M. S., Fewtrell, T. J., 2010. A simple inertial formulation of the shallow water equations for efficient two-dimensional flood inundation modelling. Journal of Hydrology 387 (1), 33–45.

Boardman, J., Evans, R., Ford, J., 2003. Muddy floods on the south downs, southern england: problem and responses. Environmental Science & Policy 6 (1), 69–83.

Booij, N., Holthuijsen, L., Ris, R., 1996. The" swan" wave model for shallow water. Coastal Engineering Proceedings 1 (25).

Brooks, S. M., Spencer, T., McIvor, A., Möller, I., 2016. Reconstructing and understanding the impacts of storms and surges, southern north sea. Earth Surface Processes and Landforms 41 (6), 855–864.

Brouwer, C., Prins, K., Kay, M., Heibloem, M., 1988. Irrigation water management: irrigation methods. Food and Agriculture Organization of the United Nations (FAO) Land and Water Development Division.

Bunney, C., Saulter, A., 2015. An ensemble forecast system for prediction of atlantic–uk wind waves. Ocean Modelling 96, 103–116.

Department for Transport, 2016. Traffic count data. Accessed 03 October 2016. URL http://www.dft.gov.uk/traffic-counts/

Destination Research, 2014. Economic impact of tourism: Norfolk 2014. Accessed 03 October 2016.
URL http://www.visitnorfolk.co.uk/Tourism-info-and-stats.aspx

Donnelly, C., 2008. Coastal overwash: processes and modelling. Lund University (Media-Tryck).

Environment Agency, 2010. North norfolk shoreline management plan, old hunstanton to kelling hard.

Environment Agency, 2014. Sea state report norfolk: Year 3 and summary for october 2006-september 2009.

Flather, R. A., 2000. Existing operational oceanography. Coastal Engineering 41 (1), 13–40.

Haigh, I. D., Wadey, M. P., Gallop, S. L., Loehr, H., Nicholls, R. J., Horsburgh, K., Brown, J. M., Bradshaw, E., 2015. A user-friendly database of coastal flooding in the united kingdom from 1915–2014. Scientific data 2.

Holman, R., 1986. Extreme value statistics for wave run-up on a natural beach. Coastal Engineering 9 (6), 527–544.

Jenks, G. F., 1967. The data model concept in statistical mapping. International yearbook of cartography 7 (1), 186–190.

Karvonen, R., Hepojoki, A., Huhta, H., Louhio, A., 2000. The use of physical models in dam-break analysis. RESCDAM Final Report. Helsinki University of Technology, Helsinki, Finland.

Lessnoff, A., 2008. Vertical Offshore Reference Frame UK Model: User Guide. United Kingdom Hydrographic Office.

Matias, A., Blenkinsopp, C. E., Masselink, G., 2014. Detailed investigation of overwash on a gravel barrier. Marine Geology 350, 27–38.

McCall, R. T., De Vries, J. V. T., Plant, N., Van Dongeren, A., Roelvink, J., Thompson, D., Reniers, A., 2010. Two-dimensional time dependent hurricane overwash and erosion modeling at santa rosa island. Coastal Engineering 57 (7), 668–683.

McLaughlin, S., Cooper, J. A. G., 2010. A multi-scale coastal vulnerability index: A tool for coastal managers? Environmental Hazards 9 (3), 233–248.

Möller, I., 2006. Quantifying saltmarsh vegetation and its effect on wave height dissipation: Results from a uk east coast saltmarsh. Estuarine, Coastal and Shelf Science 69 (3), 337–351.

Möller, I., Kudella, M., Rupprecht, F., Spencer, T., Paul, M., van Wesenbeeck, B. K., Wolters, G., Jensen, K., Bouma, T. J., Miranda-Lange, M., et al., 2014.

Wave attenuation over coastal salt marshes under storm surge conditions. Nature Geoscience 7 (10), 727–731.

Möller, I., Spencer, T., French, J., Leggett, D., Dixon, M., 1999. Wave transformation over salt marshes: a field and numerical modelling study from north norfolk, england. Estuarine, Coastal and Shelf Science 49 (3), 411–426.

Office for National Statistics (ONS), 2014. Living costs and food survey 2013. Data available to registered users from the UK Data Service website, accessed 03 October 2016.
URL https://discover.ukdataservice.ac.uk/series/?sn=2000028

Penning-Rowsell, E., Priest, S., Parker, D., Morris, J., Tunstall, S., Viavattene, C., Chatterton, J., Owen, D., 2013. Flood and Coastal Erosion Risk Management: A Manual for Economic Appraisal. London and New York, Routledge.

Penning-Rowsell, E., Priest, S., Parker, D., Morris, J., Tunstall, S., Viavattene, C., Chatterton, J., Owen, D., 2016. Flood and Coastal Erosion Risk Management: A Handbook for Economic Appraisal. Available from mcm-online.co.uk.

Priest, S. J., Wilson, T., Tapsell, S. M., Penning-Rowsell, E. C., Viavattene, C., Fernandez-Bilbao, A., 2007. Building a model to estimate risk to life for european flood events–final report.

Prime, T., Brown, J. M., Plater, A. J., 2016. Flood inundation uncertainty: the case of a 0.5% annual probability flood event. Environmental Science & Policy 59, 1–9.

Pullen, T., Allsop, N., Bruce, T., Kortenhaus, A., Sch, H., Van der Meer, J., et al., 2007. Wave overtopping of sea defences and related structures: assessment manual. Boyens Medien GmbH.

Roelvink, D., Dastgheib, A., Spencer, T., Möller, I., Christie, E., Berenguer, M., Semper-Torres, D., 2015. Deliverable d3.2: Updated physical models. Tech. rep., RISC-KIT.

Roelvink, D., Reniers, A., Van Dongeren, A., de Vries, J. v. T., McCall, R., Lescinski, J., 2009. Modelling storm impacts on beaches, dunes and barrier islands. Coastal engineering 56 (11), 1133–1152.

Roelvink, D., Reniers, A., Van Dongeren, A., Van Thiel de Vries, J., Lescinski, J., McCall, R., 2010. Xbeach model description and manual. Delft University of Technology, User Manual, Delft, The Netherlands.

Royal Society for the Protection of Birds (RSPB), 2000. Valuing norfolks coast. Accessed 03 October 2016.
URL https://www.rspb.org.uk/Images/Valuing_norfolks_coast_tcm9-203973.pdf

Sallenger Jr, A. H., 2000. Storm impact scale for barrier islands. Journal of Coastal Research, 890–895.

Schüttrumpf, H., Oumeraci, H., 2005. Layer thicknesses and velocities of wave overtopping flow at seadikes. Coastal Engineering 52 (6), 473–495.

Scottish Widows, 2014. Press release: People with no nest egg rises to over 9 million as gap between savers and non-savers widens. 6 march 2014. Accessed 03 October 2016.
URL http://reference.scottishwidows.co.uk/literature/doc/2014-03-SavingsReport

Spencer, T., Brooks, S. M., Evans, B. R., Tempest, J. A., Möller, I., 2015. Southern north sea storm surge event of 5 december 2013: water levels, waves and coastal impacts. Earth-Science Reviews 146, 120–145.

Steers, J., Stoddart, D., Bayliss-Smith, T., Spencer, T., Durbidge, P., 1979. The storm surge of 11 january 1978 on the east coast of england. Geographical Journal, 192–205.

Stockdon, H. F., Holman, R. A., Howd, P. A., Sallenger, A. H., 2006. Empirical parameterization of setup, swash, and runup. Coastal engineering 53 (7), 573–588.

Tapsell, S. M., Penning-Rowsell, E. C., Tunstall, S. M., Wilson, T., 2002. Vulnerability to flooding: health and social dimensions. Philosophical Transactions of the Royal Society of London A: Mathematical, Physical and Engineering Sciences 360 (1796), 1511–1525.

The South West Research Company, 2014. The economic impact of the norfolk visitor economy 2012: North norfolk district and norfolk county. Accessed 03 October 2016.
URL https://www.northnorfolk.org/files/Value_Volume_study.pdf

Torresan, S., Critto, A., Dalla Valle, M., Harvey, N., Marcomini, A., 2008. Assessing coastal vulnerability to climate change: comparing segmentation at global and regional scales. Sustainability Science 3 (1), 45–65.

Torresan, S., Critto, A., Rizzi, J., Marcomini, A., 2012. Assessment of coastal vulnerability to climate change hazards at the regional scale: the case study of the north adriatic sea. Natural Hazards and Earth System Sciences 12 (7), 2347–2368.

Viavattene, C., Jimenez, J. A., Owen, D., Priest, S., Parker, D., Micou, A. P., Ly, S., 2015. Deliverable d2.3: Coastal risk assessment framework guidance document. Tech. rep., RISC-KIT.

Viavattene, C., Priest, S. J., Owen, D., Parker, D. J., Micou, P., Ly, S., 2016. Indra model: for a better assessment of coastal events disruptions. In: ISCRAM 2016 proceedings.